First direct lifetime measurement of the 2_1^+ state in ^{72,74}Zn: New evidence for a shape transition between $N = 40$ and $N = 42$ close to $Z = 28$

M. Niikura,[1,*] B. Mouginot,[1] S. Franchoo,[1] I. Matea,[1] I. Stefan,[1] D. Verney,[1] F. Azaiez,[1] M. Assie,[1,2] P. Bednarczyk,[3] C. Borcea,[4] A. Burger,[5] G. Burgunder,[2] A. Buta,[4] L. Cáceres,[2] E. Clément,[2] L. Coquard,[6] G. de Angelis,[7] G. de France,[2] F. de Oliveira Santos,[2] A. Dewald,[8] A. Dijon,[2] Z. Dombradi,[9] E. Fiori,[10] C. Fransen,[8] G. Friessner,[8] L. Gaudefroy,[11] G. Georgiev,[10] S. Grévy,[2] M. Hackstein,[8] M. N. Harakeh,[2,12] F. Ibrahim,[1] O. Kamalou,[2] M. Kmiecik,[3] R. Lozeva,[10,13] A. Maj,[3] C. Mihai,[4] O. Möller,[6] S. Myalski,[3] F. Negoita,[4] D. Pantelica,[4] L. Perrot,[1] Th. Pissulla,[8] F. Rotaru,[4] W. Rother,[8] J. A. Scarpaci,[1] C. Stodel,[2] J. C. Thomas,[2] and P. Ujic[2,14]

[1]*Institut de Physique Nucléaire (IPN), IN2P3-CNRS, Université Paris-Sud 11, F-91406 Orsay Cedex, France*
[2]*Grand Accélérateur National d'Ions Lourds (GANIL), CEA/DSM-CNRS/IN2P3, BP 55027, F-14076 Caen Cedex 05, France*
[3]*The Henryk Niewodniczański Institute of Nuclear Physics (IFJ PAN), PL-31342 Kraków, Poland*
[4]*Horia Hulubei National Institute for Physics and Nuclear Engineering (IFIN-HH), P.O. Box MG-6, ROM-76900 Bucharest-Magurele, Romania*
[5]*Department of Physics, University of Oslo, N-0315 Oslo, Norway*
[6]*Institut für Kernphysik, der Technische Universität Darmstadt, D-64289 Darmstadt, Germany*
[7]*Laboratori Nazionali di Legnaro, INFN, I-35020 Legnaro, Padova, Italy*
[8]*Institut für Kernphysik, Universität zu Köln, Zülpicher Straße 77, D-50937 Köln, Germany*
[9]*Institute of Nuclear Research of the Hungarian Academy of Sciences (ATOMKI), P.O. Box 51, H-4001 Debrecen, Hungary*
[10]*CSNSM, UMR 8609, IN2P3-CNRS, Université Paris-Sud 11, F-91405 Orsay Cedex, France*
[11]*CEA, DAM, DIF, F-91297 Arpajon, France*
[12]*Kernfysisch Versneller Instituut (KVI), University of Groningen, NL-9747 AA Groningen, The Netherlands*
[13]*IPHC, IN2P3-CNRS, Université de Strasbourg, F-67037 Strasbourg, France*
[14]*Vinca Institute of Nuclear Sciences, University of Belgrade, Nos. 12–14 Mike Alasa, 11001 Vinca, Serbia*

(Received 24 May 2011; revised manuscript received 13 February 2012; published 31 May 2012)

We report here the first direct lifetime measurement of the 2_1^+ state in ^{72,74}Zn. The neutron-rich beam was produced by in-flight fragmentation of ^{76}Ge at the Grand Accélérateur National d'Ions Lourds and separated with the LISE spectrometer. The 2_1^+ state was excited by inelastic scattering and knock-out reaction on a CD_2 target and its lifetime was measured by the recoil-distance Doppler-shift method with the Köln plunger device combined with the EXOGAM detectors. The lifetimes of the 2_1^+ states in ^{72,74}Zn were determined to be 17.9(18) and 27.0(24) ps, which correspond to reduced transition probabilities $B(E2; 2_1^+ \rightarrow 0^+) = 385(39)$ and 370(33) e^2 fm^4, respectively. These values support the idea of a systematic maximum of collectivity at $N = 42$ for Zn, Ge, and Se nuclei. In addition, the available systematics in the neighboring nuclei point toward a transition from a spherical oscillator at $N = 40$ to complete γ-softness at $N = 42$.

DOI: 10.1103/PhysRevC.85.054321 PACS number(s): 21.10.Tg, 23.20.Lv, 25.70.Mn, 27.50.+e

I. INTRODUCTION

There has been continuous interest in the study of the structure effects associated with $N = 40$ close to $Z = 28$ since the original publication by Bernas *et al.* [1] and the magic character of $^{68}_{28}$Ni$_{40}$ has been extensively discussed (for instance, see Ref. [2] and references therein). One of the most interesting features in the immediate vicinity of the $Z = 28$, $N = 40$ crossing was pointed out by Perru *et al.* [3] and consists in an apparent overoccupation of the neutron $1g_{9/2}$ orbit, starting already for $N \leqslant 40$, and a concomitant strong proton core polarization effect. These phenomena were invoked to explain the sudden and large increase of a reduced transition probability $B(E2)$ observed between ^{68}Ni$_{40}$ and ^{70}Ni$_{42}$. Independently, there has been considerable accumulation of experimental evidence pointing toward a sudden structural change from $N = 40$ to 42 in the Ge chain. This change was originally inferred from the analysis of nucleon transfer cross sections [4] and was seen to be also present in the Se chain [5] though somewhat attenuated. This phenomenon is also clear when considering $B(E2)$ and $Q(2_1^+)$ data [6]. It was soon admitted that the Ge and Se nuclei undergo a maximum of collectivity (in the most general sense) at $N = 42$ [6–8] and that a new collectivity regime (the nature of which will be discussed in last section) develops at this particular neutron number to the end of the neutron $1g_{9/2}$ shell. From the comparison with Ge and Se systematics one could naturally expect a maximum of collectivity at $N = 42$, or more generally structural change from $N = 40$ to 42, also in the Zn chain. In addition, the microscopic mechanism that would connect the strong polarization effect affecting the $B(E2)$ value in ^{70}Ni$_{42}$ to the $N = 42$ collectivity maximum in Ge and Se is still difficult to establish in a direct way. The overoccupation of the neutron $1g_{9/2}$ orbit for $Z \geqslant 30$, already hinted at in Ref. [3], is confirmed by recent shell-model calculations [9]: this can be seen, for instance, in Fig. 24 of Ref. [9], which shows calculated occupation of the neutron

*niikura@ipno.in2p3.fr

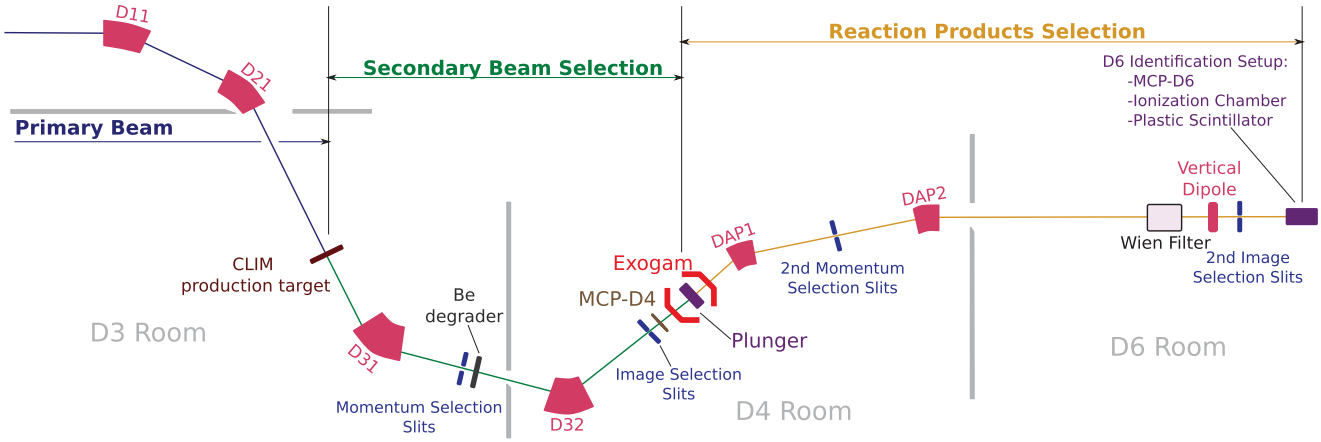

FIG. 1. (Color online) Schematic view of the experimental setup. In this measurement LISE was used both for secondary-beam selection (rooms between D3 and D4) and for reaction-products selection from secondary target (rooms between D4 and D6). The secondary beam was produced in the CLIM production target [16,17] installed in D3. The Köln plunger device [18] was placed at the first achromatic focal point (D4), surrounded by eight EXOGAM clovers. A ΔE-E telescope consisting of an ionization chamber and a plastic scintillator was placed in D6.

$1g_{9/2}$ orbit in the 0_g^+ and 2_g^+ states of the even-even Ge chain. However, in these calculations the proton $1f_{7/2}$ orbit is not included in the valence space and the effect of the proton core polarization cannot be quantified directly; i.e., if such an effect is indeed accounted for, it is only through a very indirect way, that is, via some modification of the residual interaction after fitting some of the two-body matrix elements to data on nuclei close to $Z = 28$. More recently, shell-model calculations in a larger valence space including the fp shell for protons and the $1f_{5/2}$, $2p_{3/2}$, $2p_{1/2}$, $1g_{9/2}$, and $2d_{5/2}$ orbitals for neutrons became available [10]. The strong increase of $B(E2)$ values from ^{68}Ni$_{40}$ to ^{70}Ni$_{42}$ is somewhat reproduced using standard effective charges but not quite (see Fig. 5 in Ref. [10]). Interestingly, a second calculation in the same valence space but with a slightly revised version of the residual interaction worsens a little bit the result [11], as if the inclusion of the $\Delta\ell = 2$ quadrupole partners $g_{9/2}$-$d_{5/2}$, contrary to what had been expected earlier, was not a sufficient ingredient to explain the apparent increase of "collectivity" in Ni between $N = 40$ and 42. Even-even Zn nuclei close to $N = 40$ should then provide the ideal test ground if one is to try to pin down the potential connection between the two phenomena: strong proton core polarization and maximum collectivity at $N = 42$.

In this paper we propose to address this question by means of a direct lifetime measurement of the 2_1^+ state in ^{72}Zn$_{42}$ and ^{74}Zn$_{44}$. We expect in that way to get a more accurate evaluation of the $B(E2)$ values than those obtained from the previous scattering cross-section measurements [3,12,13], which are generally sensitive to the energy regime and/or model dependent in some way. In particular, when not all the $E2$ strength connecting the lowest-lying states can be observed—which is usually the case in radioactive beam experiments—some value for the quadrupole moment of the 2^+ state must be assumed. This kind of assumption is particularity hazardous in a region of transitional nuclei characterized by subtle and complicated collective effects.

II. EXPERIMENTAL CONDITIONS

The experiment was performed at the Grand Accélérateur National d'Ions Lourds (GANIL) using the recoil-distance Doppler-shift method (RDDS) method [14] applied to the intermediate-energy reaction. The LISE spectrometer [15] was used both for the separation of the reaction fragments in the first half of the spectrometer and for the identification of the reaction recoils in the second half. Details of the experimental setup are shown in Fig. 1.

A cocktail beam of ^{73,74}Zn and ^{72}Cu was produced by the projectile-fragmentation reaction of a 60-MeV/nucleon ^{76}Ge^{30+} beam impinging on the CLIM device [16,17] consisting of a 580-μm-thick ^{9}Be target. A 500-μm-thick ^{9}Be wedge degrader was placed in the first dispersive focal plane of LISE to select nuclei of interest produced in the target. A total average intensity of 1.0×10^5 particles per second containing 75%^{74}Zn was measured at D4 with 1.0 $e\mu$A of the primary beam intensity.

The Köln plunger device [18] used for the RDDS measurement was mounted with a 445-μm-thick (35.5-mg/cm^2) CD_2 target and a 273-μm-thick (50.5-mg/cm^2) ^{9}Be degrader at the first achromatic focal point of LISE (D4). The distance between the target and the degrader can be varied by changing the degrader position with a relative precision of 5 μm. In the present experiment ten different target-degrader distances (d) were set over the range from 0 to 20 mm as summarized in Table I. The plunger device was surrounded by eight segmented EXOGAM Ge clovers [19–21], covering angles between 30° and 58° and between 117° and 148° with respect to the beam direction. The electronic segmentation of the EXOGAM clovers reduces the Doppler broadening by about 40%, leading to a full width at half maximum (FWHM) energy resolution of about 15 keV for the 605.9-keV $2_1^+ \rightarrow 0^+$ transition in ^{74}Zn.

The identification of the nuclei was carried out by means of energy loss and time-of-flight (ΔE-TOF) measurements. ΔE was measured with an ionization chamber (CHIO) placed

TABLE I. Summary of total statistics accumulated and measured decay curve $[I'_a/(I'_b + I'_a)]$ in each of the ten target-degrader distances (d). Distances presented here were measured between the back side of the target and the front side of the degrader.

d (mm)	Statistics	$I'_a/(I'_b + I'_a)$	
		^{72}Zn	^{74}Zn
0.00	27114810	—	—
0.75	31411531	0.895(20)	0.914(25)
1.25	34776072	0.758(35)	0.858(13)
1.75	37650948	0.699(16)	0.757(13)
2.50	44109130	0.569(23)	0.695(10)
3.50	30070949	0.597(26)	0.621(11)
5.00	38184414	0.489(20)	0.564(13)
8.00	31748616	0.510(25)	0.509(11)
15.0	18374052	0.524(59)	0.499(20)
20.0	25005851	0.475(31)	0.509(22)

at the final achromatic focal point of LISE (D6) in front of a plastic scintillator. The TOF was measured between two microchannel plate detectors (MCPs) [22]: the first one was placed 1.107 m upstream of the plunger device, and the second one was installed in front of the ionization chamber. They allowed an accurate TOF measurement for the recoil fragments between D4 and D6 (distance = 24.739 m). The efficiencies of the MCPs were about 90% and 95% for D4 and D6, respectively. The typical count rate in the D6 detectors was 1.0×10^4 counts per second.

The acquisition was triggered mainly by the coincidence between the plastic scintillator in D6 and one or more EXOGAM detectors. The coincidence window was set to 200 ns. About 3×10^7 triggered events were corrected for each target-degrader distance setting, as summarized in Table I.

III. ANALYSIS PROCEDURE AND RESULTS

The lifetime of the 2_1^+ state in ^{72,74}Zn was deduced based on the differential decay curve (DDC) method [14] applied for the intermediate-energy reaction. To apply the DDC method, the decay curve $I_a/(I_b + I_a)$ has to be obtained from γ-ray spectra, where I_b and I_a are the intensities of the γ rays emitted before and after the degrader from the 2_1^+ state of ^{72,74}Zn excited in the target.

In the present experiment, reactions in the degrader can also produce the excited state of interest. Therefore, the extracted intensities from the measured γ spectra are not I_b and I_a, but I'_b and I'_a. I'_b represents the number of decays from the 2_1^+ state before the degrader; therefore $I_b = I'_b$. On the other hand, I'_a is the total number of decays after the degrader from the 2_1^+ state. Therefore, $I'_a = I_a + I_{deg}$, where I_{deg} represents the decays from the 2^+ state produced in the degrader. The decay curve can be extracted as

$$\frac{I_a}{I_b + I_a} = (1 + \alpha)\frac{I'_a}{I'_b + I'_a} - \alpha, \quad (1)$$

with the production ratio between the degrader and the target defined as $\alpha = I_{deg}/(I_b + I_a)$. In the case of a sufficiently long distance between the target and the degrader, one can assume $I_a \simeq 0$ and the α constant can be deduced from Eq. (1) as

$$\alpha = I'_a/I'_b. \quad (2)$$

Figure 2 shows the Doppler-corrected γ-ray spectra measured for the three different emission angles of the γ rays (θ) used in the Doppler correction and at three out of ten target-degrader distances. For the lifetime determination only forward EXOGAM detectors were used due to a 511-keV contamination in the spectra of the backward detectors. From the forward-angle detectors, segments with angles between 51° and 58° were removed from the analysis due to the poor separation between the peaks of interest.

The geometrical efficiencies as a function of the γ-ray emission point and the γ-ray energies as well as their widths detected in EXOGAM were determined by a GEANT4 simulation [23,24]. The simulation takes into account the velocities of the incoming and outgoing particles, the energy losses through the target and degrader, and the detector geometry. Isotropic γ-ray emission with the Lorentz boost effect and a given lifetime are assumed in the event generator of the simulation. Therefore, a line-shape effect of the γ peaks is naturally included.

The intensities of the γ rays emitted before and after the degrader from the 2_1^+ state of ^{72,74}Zn (I'_b and I'_a) were extracted by fitting the region of interest with four Gaussian functions as shown in Fig. 2. The mean and sigma values for the Gaussian functions are fixed from the simulation using mean velocities between target and degrader ($\beta = v/c$) of 0.2449(11) and 0.2433(11) for ^{72}Zn and ^{74}Zn, respectively. These β values were obtained from the alignment of Doppler-corrected peaks at all measured angles. Obtained intensity ratios $I'_a/(I'_b + I'_a)$, after taking into account the geometrical efficiencies, are shown in Table I.

The α constants were extracted by means of Eq. (2) and were found to be 1.00(7) and 1.01(6) for ^{72}Zn and ^{74}Zn, respectively. The largest three distances (8.0, 15.0, and 20.0 mm) for ^{72}Zn and two (15.0 and 20.0 mm) for ^{74}Zn were used for this α constant extraction. Figure 3 shows the result of the DDC method applied to the decay curve obtained with Eq. (1). The lifetimes were deduced to be 17.9(18) and 27.0(24) ps for ^{72}Zn and ^{74}Zn, respectively. The errors are dominated by the error on the α parameter (1.7 and 2.3 ps).

The side-feeding contribution to the lifetime from excitation of higher energy states was examined. The upper limit of the 4_1^+ population was obtained to be 30% of the 2_1^+ state population from the intensity of the 847- (^{72}Zn) and 812-keV (^{74}Zn) $4_1^+ \rightarrow 2_1^+$ transition in the γ-ray spectra. As long as the lifetime of the 4_1^+ state is estimated to be less than 3 ps [13], none of the data points at distances in the sensitive region for the DDC method are affected by the side feeding. No other γ lines have been observed in γ-γ coincidence spectra gated on the 2_1^+ decay of ^{72,74}Zn.

The obtained lifetimes of 17.9(18) and 27.0(24) ps correspond to reduced transition probabilities $B(E2; 2_1^+ \rightarrow 0^+) =$ 385(39) and 370(33) e^2 fm^4 for ^{72}Zn and ^{74}Zn, respectively. These values are comparable within error bars to ones extracted from Coulomb-excitation experiments with intermediate- and low-energy ^{72,74}Zn beams, which give $B(E2)$ values of

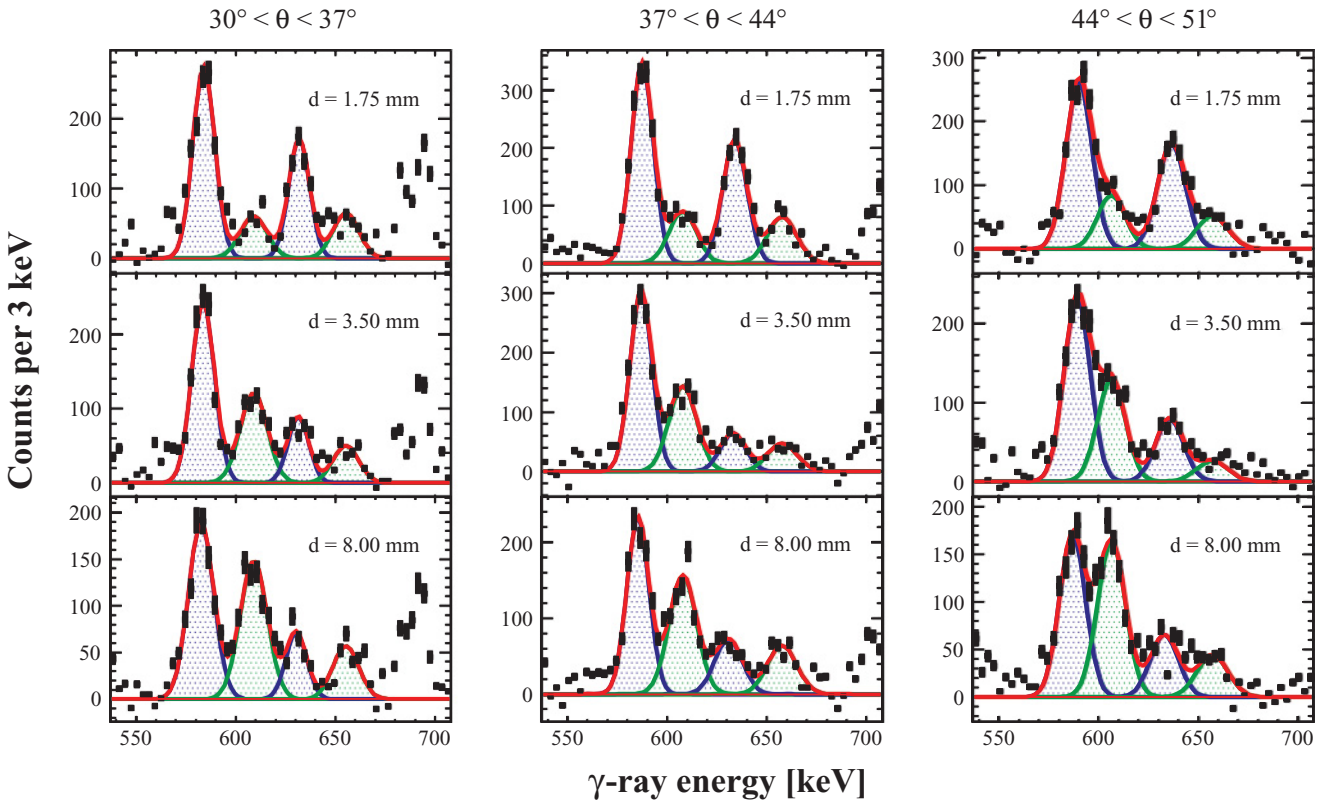

FIG. 2. (Color online) Measured γ-ray spectra after Doppler correction and background subtraction. They are gated on the prompt γ timing within 10 ns. The four photopeaks observed in the spectra are associated with the $2_1^+ \rightarrow 0^+$ transitions of ^{74,72}Zn corresponding to the different recoil velocities before and after the degrader, respectively. Solid lines represent the results of fitting with the Gaussian functions parametrized by a GEANT4 simulation. Gamma peaks shown in the range 680–700 keV at small angles are contaminants from ^{72}Ge(n, n') (at 834 keV in the laboratory coordinate system).

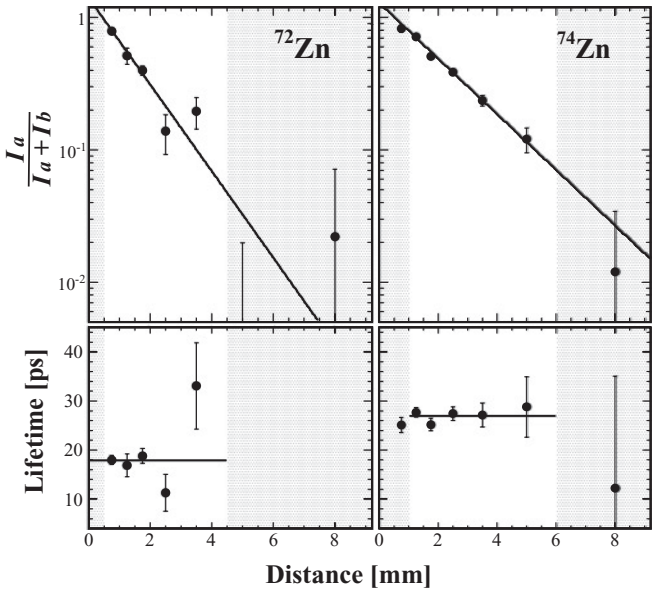

FIG. 3. Decay curves $[I_a/(I_b + I_a)]$ (top) and lifetimes (bottom) of the 2_1^+ state in ^{72,74}Zn (left and right) at several target-degrader distances. Decay curves are plotted on a logarithmic scale. Points in the grayed areas are out of the "region of sensitivity" for the DDC method [14].

348(42) e^2 fm^4 (for ^{72}Zn) [12] and 408(30) and 401(32) e^2 fm^4 (for ^{74}Zn) [3,13]. As can be seen in Fig. 4, our value for ^{72}Zn is closer to the higher tip of the error bar, whereas for ^{74}Zn it is closer to the lower tip. The $B(E2)$ systematics with new values obtained in the present work shows a similar trend with that of Ge and Se nuclei, which have the same local maximum at $N = 42$. The consequence of this trend will be discussed in the forthcoming section. In the previous work on ^{74}Zn [13], the $B(E2)$ value was obtained using the GOSIA code on the assumption of the spectroscopic quadrupole moment $Q(2_1^+) = 0$ e b and the authors also provide a correlation between the lifetime and $Q(2_1^+)$ (see Fig. 9 in Ref. [13]). From the comparison between the present data and the previous Coulex measurement a value of $Q(2_1^+) = +0.22(30)$ e b can be extracted for ^{74}Zn. The obtained $Q(2_1^+)$ of ^{74}Zn will be also discussed in the next section.

IV. DISCUSSION

A. Structural transition from $N = 40$ to 42

In a first attempt to understand the development of collectivity in the even-even Zn chain and to help in determine its nature, it is interesting to consider the Zn data within

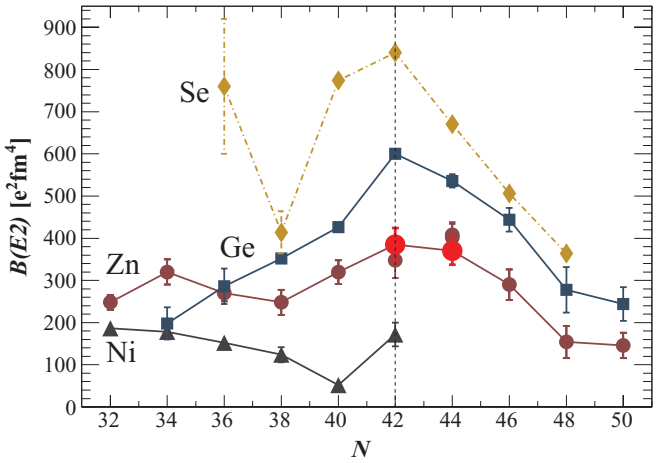

FIG. 4. (Color online) Experimental systematics of $B(E2)$ for Ni (triangles), Zn (filled circles), Ge (squares), and Se (diamonds) isotopes. The values obtained within the present work are superimposed in red.

the regional systematics. The energies of the first 2^+ states versus neutron number for $30 \leqslant Z \leqslant 38$ even-even nuclei are shown in Fig. 5. Two groups with different behavior can be distinguished at once: $E(2_1^+)$ is minimum for Sr and Kr close or at $N = 38$, while there is a maximum for Zn and Ge for exactly the same number of neutrons. As already pointed out some time ago [25] this region provides a nice illustration of the concepts of reinforcing and switching of shell gaps: the second group ("S group") appears indeed to be dominated by $N = 38$–40 fragile spherical gaps, reinforced by the proximity of the $Z = 28$ strong spherical gap, while the first ("D group") appears to be dominated by the mutual reinforcement of $Z, N = 38$ deformed gaps. The Se chain would correspond to some transition between the two regimes. Figure 6 shows the measured $Q(2_1^+)$ values as a function of neutron number for Zn, Ge, and Se: globally, some transition is observed at $N \simeq 40$, from smaller absolute values (including one compatible with 0), to larger absolute values that are, however, all negative.

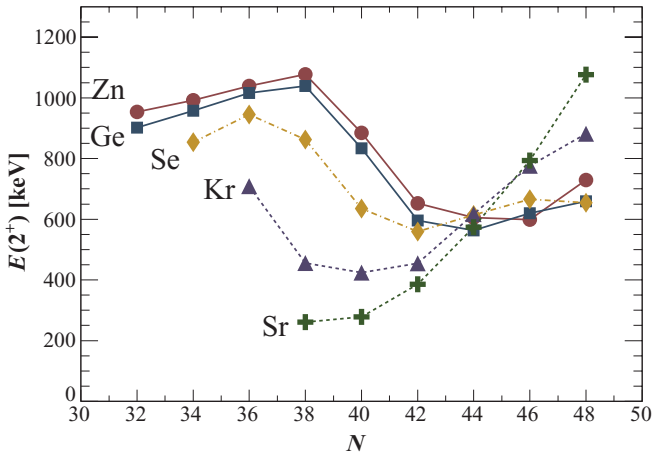

FIG. 5. (Color online) Energy of the first 2^+ state of Zn (filled circles), Ge (squares), Se (diamonds), Kr (triangles), and Sr (crosses) nuclei.

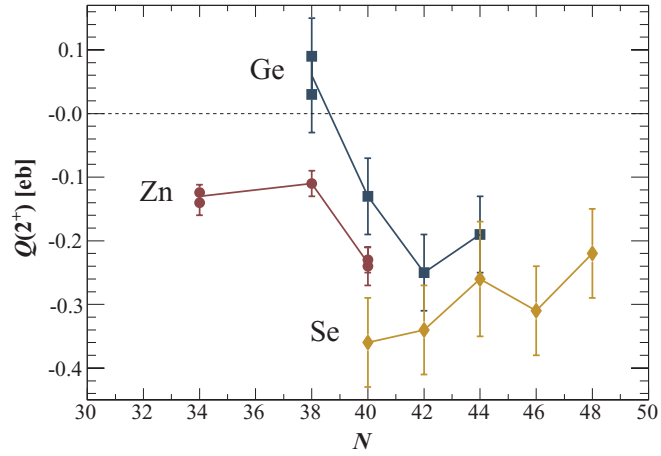

FIG. 6. (Color online) Measured $Q(2_1^+)$ (e b) values for Zn (filled circles), Ge (squares), Se (diamonds), Kr (triangles), and Sr (crosses) nuclei [27].

At $N = 40$, the value for Zn gets closer to those for Se, characteristic of a more prolate *average* intrinsic shape. We note that no measured $Q(2_1^+)$ is compatible with an intrinsic oblate shape for $N \geqslant 40$ for any of the three isotopic chains.

It is interesting to consider also the inertia parameters $A = \hbar^2/2\Im$ corresponding to the $6_1^+ - 4_1^+$ energy differences (which allows us to get rid of band-mixing effects to some extent). These values are reported in Fig. 7 as a function of the neutron number. The largest value for the moment of inertia is found at $N = 38$ for $Z = 34$ and $Z = 36$. By contrast, for both $Z = 30$ and 32 the moment of inertia increases up to $N = 40$ and then is somewhat stabilized with values of the inertia parameter $A = \hbar^2/2\Im$ scattered around 50 keV, hinting at the apparent stabilization of a certain dynamic regime from $N = 40$ and all along the $\nu 1g_{9/2}$ filling.

An additional piece of information which documents a maximum of quadrupole coherence at $N = 42$ is provided by the energy systematics of the first $9/2^+$ states versus neutron

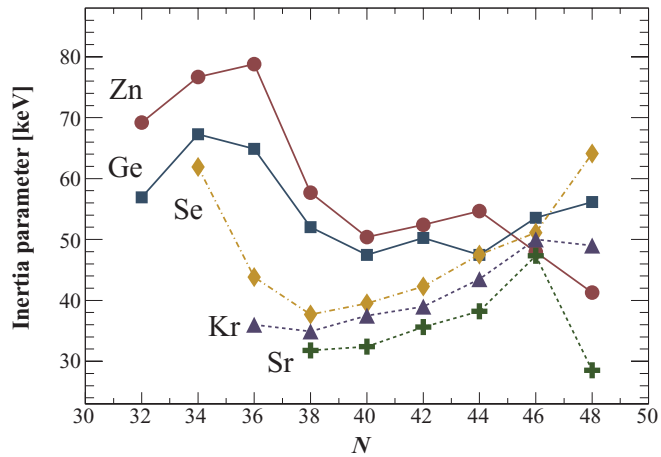

FIG. 7. (Color online) Parameter of inertia $A = \hbar^2/2\Im$ from the $6^+ \rightarrow 4^+$ experimental energies for Zn (filled circles), Ge (squares), Se (diamonds), Kr (triangles), and Sr (crosses) nuclei (with 6^+ energies for ^{74,76}Zn taken from an unpublished work [26]).

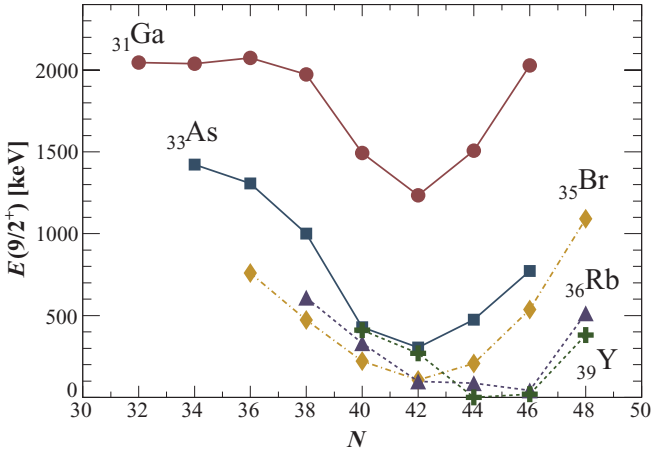

FIG. 8. (Color online) Energy of the first $9/2^+$ state in the odd-proton Ga (filled circles), As (squares), Br (diamonds), Rb (triangles), and Y (crosses) nuclei.

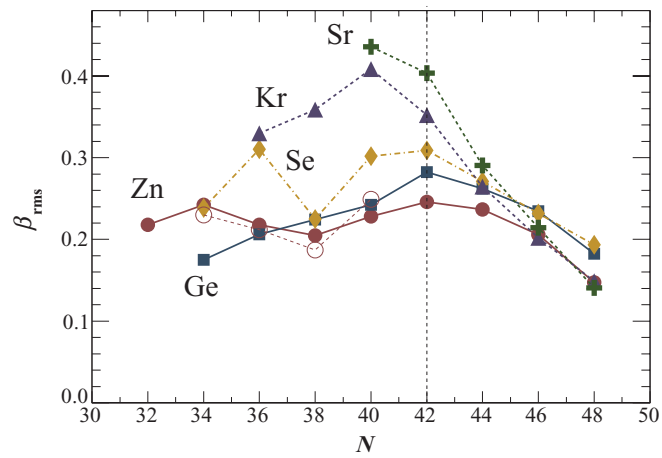

FIG. 9. (Color online) Root-mean-square (rms) deformation parameters for Zn (filled circles), Ge (squares), Se (diamonds), Kr (triangles), and Sr (crosses) nuclei. [No error bars are reported here due to the intrinsic uncertainty of Eq. (3).] β_2 experimental values for Zn [29] are represented by open circles.

number for $31 \leqslant Z \leqslant 39$ odd-even nuclei as shown in Fig. 8. These states are interpreted, on the oblate side, as the head of the band built on the rapidly down-sloping $9/2^+[404]$ Nilsson orbital stemming from the proton $1g_{9/2}$ spherical orbit, or, alternately, on the slightly prolate side, as the favored members of a rotation aligned band built on the $1/2^+[440]$ Nilsson orbital stemming from the same shell. One sees that these opposite parity states have a minimum in energy at $N = 42$ for Ga (Zn +1 proton), As (Ge + 1 proton), and Br (Se + 1 proton).

Finally, the new values of the reduced transition probability $B(E2; 2_1^+ \rightarrow 0^+)$ for ^{72,74}Zn obtained from the present work, when inserted in the existing systematics (see Fig. 4), allow us to confirm the same interesting feature: the maximum value for Zn, Ge, and Se is reached systematically at $N = 42$. As is well known, the most probable deformation parameter can be evaluated by

$$\beta_{\rm rms} \gtrsim \frac{4\pi\sqrt{5}}{3ZR_0^2}\sqrt{B(E2; 2_1^+ \rightarrow 0^+)}, \qquad (3)$$

with $R_0 = 1.2A^{1/3}$ fm. This relation, which was originally derived by Kumar [28], is model independent in the sense that no intrinsic shape is assumed; the only assumption is a uniform charge distribution inside a sharp oscillating surface. This quantity is a measure of the collectivity in general: large values of $\beta_{\rm rms}$ should be understood as an indication of large deformation or big vibration amplitudes or both. Only in the case of a permanent axially deformed intrinsic shape does all collectivity amount to the rotation of the shape and $\beta_{\rm rms} \equiv \beta_2$. An application of this relation was made by Nolte *et al.* for this mass region [7]; we present the updated systematics in Fig. 9. The β_2 parameter has been deduced in an independent way from inelastic electron-scattering cross-section measurements for $^{64-70}$Zn [29], and the values are also reported in Fig. 9. A nice agreement is found both in order of magnitude and tendency versus neutron number. From Fig. 9, a maximum of collectivity at $N = 42$ for Zn, Ge, and Se is confirmed. The question is now: Which kind of collectivity?

To answer this question a closer inspection of the energy systematics of the low-lying levels of the Zn isotopes *and* a comparison with Ge is necessary. The energy evolution as a function of neutron number for the $0^+_{2,3}$, $2^+_{1,2}$, 3^+_1, $4^+_{1,2}$, and 6^+_1 states (when identified) in Zn and Ge is drawn in Figs. 10(a) and 10(b). The trends of the structures of even-even Zn and Ge nuclei show remarkable resemblance, especially the 2^+_1 and 4^+_1 sequences. This goes along with our previous remarks that these two isotope series are the best representatives of the "S group." Figures 11(a) and 11(b) show the $R_{42} = E(4^+_1)/E(2^+_1)$ and $R_{22} = E(2^+_2)/E(2^+_1)$ ratios. The R_{42} values lie in between the values of 2 for a vibrator and 2.67 for an asymmetric rotor (Davydov-Filippov) with $\gamma = 30^\circ$, and several are compatible with the completely γ-soft [Wilets-Jean (W-J) or O(6) in the interacting boson model (IBM)representation] limit of 2.5. In any case, all remain far away from the rotor value 3.33. R_{22} always keeps modest values hinting at $\gamma_{\rm rms} \simeq 30^\circ$ and γ-softness rather than developed axially asymmetric shape. A similar conclusion was reached in Ref. [13] from the consideration of the R_{42} and $B(E2; 4^+ \rightarrow 2^+)/B(E2; 2^+ \rightarrow 0^+)$ systematics. In addition, it is interesting to note that the closest values to the spherical vibrator limit are found for both R_{42} and R_{22} for both Zn and Ge at $N = 40$. From $N = 40$ to 42, either one of the two values (or both) deviates immediately from this limit, which is never approached again for $N \geqslant 42$. Finally, Fig. 11(c) shows the signature $S(432)$ as defined by Zamfir and Casten [30],

$$S(432) = \frac{[E(4^+_\gamma) - E(3^+_\gamma)] - [E(3^+_\gamma) - E(2^+_\gamma)]}{E(2^+_1)}, \qquad (4)$$

as a means to distinguish between γ-unstable and triaxial rotor and a way to quantify $\gamma_{\rm rms}$. For the Zn even-even isotopes, these values can be interpreted as γ-softness with $\gamma_{\rm rms} \simeq 15^\circ$–$20^\circ$ for $N \leqslant 38$, quasiharmonic vibrator at $N = 40$, and complete γ-softness at $N = 42$ ($\gamma_{\rm rms} = 30^\circ$). The complete γ-softness in ^{72}Zn is confirmed by the inspection of the level scheme: there is a clear clustering of the $(2^+_2, 4^+_1)$ states

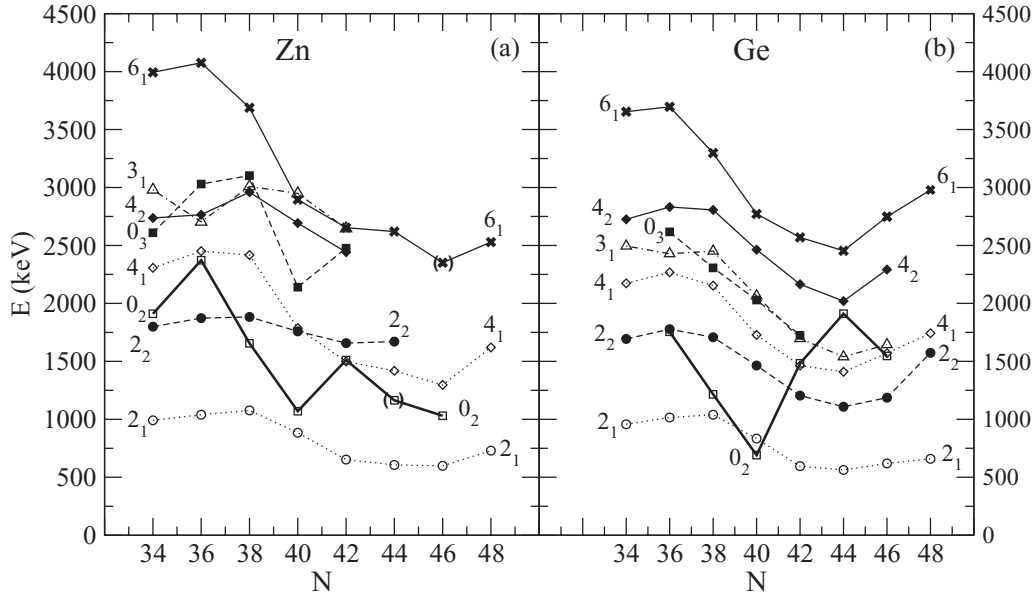

FIG. 10. Systematics of the low-lying positive-parity states in $^{64-78}$Zn and $^{66-80}$Ge. 6^+ energies for ^{74,76}Zn and ^{76}Ge were taken from an unpublished work [26].

and $(0_2^+, 3_1^+, 4_2^+, 6_1^+)$ states close to the expected energies of $2.5E(2_1^+)$ and $4.5E(2_1^+)$, respectively. In the case of the latter cluster of states, one should keep the 0_2^+ state observed at 1499 keV out of it; otherwise, this could lead to the fake picture of a harmonic vibrator. It has been shown indeed that the 0_2^+ state in Ge is characterized by a markedly different structure (sometimes referred to as an "intruder") with respect to other low-lying levels: this has been abundantly discussed in the past as well as recently [8,31–37] (and references therein). Strong similitudes are observed between the Zn and Ge chains in the global trends of this 0_2^+ state for both energy evolution (Fig. 10) and reaction cross-section ratios $\sigma_{0_2^+}/\sigma_{0_{gs}^+}$ [8,38] which hint at a similar situation of coexisting structures in Zn. For instance, the measured $E0$ transition probability for the $0_2^+ \rightarrow 0_{gs}^+$ transition in ^{70}Zn ($N = 40$) is absolutely incompatible with the vibrational picture [39]. In ^{70}Zn, the 0_3^+ state is visibly pushed away by the interaction with this "intruder" state from an otherwise perfectly clustered two-phonon triplet of states that one would naturally expect from all signatures R_{42}, R_{22}, and $S(432)$ as discussed above. We note in passing that the nonzero measured $Q(2_1^+)$ value for ^{70}Zn (see Fig. 6) is *not* in contradiction with the harmonic picture since, even in a nucleus whose equilibrium shape is spherical, the cubic term can lead to a pseudorotational value for the static quadrupole moment $Q(2_1^+)$.

In conclusion, the $B(E2)$ values for ^{72,74}Zn obtained in the present work introduce a change in the global trend of the Zn $B(E2)$ systematics which brings new support to the idea of a maximum of collectivity at $N = 42$ for the S group in the $f_{5/2}pg_{9/2}$ shell. All experimental evidence points toward a transition from a spherical oscillator at $N = 40$ to complete γ-softness at $N = 42$. Only the missing knowledge of any $B(E2)$ ratios prevents us from designating definitely ^{72}Zn as a textbook example of a Wilets-Jean [or O(6) in IBM language] γ-soft nucleus. In the complete γ-unstable picture, $Q(2_1^+)$ is identically zero. At $N = 44$, γ-softness apparently persists (from R_{42}, R_{22} of Fig. 11 and $B(E2)$ ratios as shown in Fig. 11 of Ref. [13]), which means that $Q(2_1^+)$ would remain close to zero. In view of the present discussion, the assumption of $Q(2_1^+)_{^{74}\mathrm{Zn}} = 0$ made in Ref. [13] appears as a reasonable approximation. Our $\tau_{2_1^+}$ value for ^{74}Zn is then compatible with the Coulomb-excitation data of Ref. [13] (see Fig. 9 in this reference), considering our error bars. Those data appear to

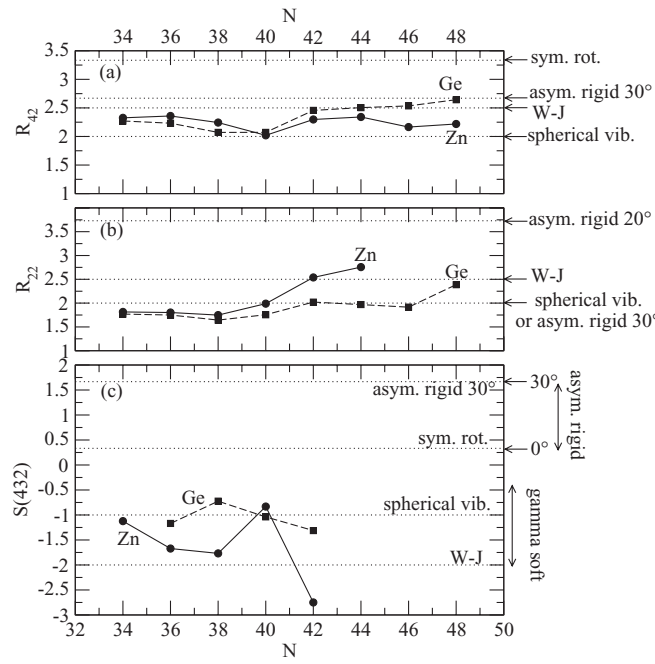

FIG. 11. Systematics of the $R_{42} = E(4_1^+)/E(2_1^+)$ and $R_{22} = E(2_2^+)/E(2_1^+)$ ratios and $S(432)$ signatures for Zn and Ge nuclei. On the right, the limits for the different geometrical models are indicated.

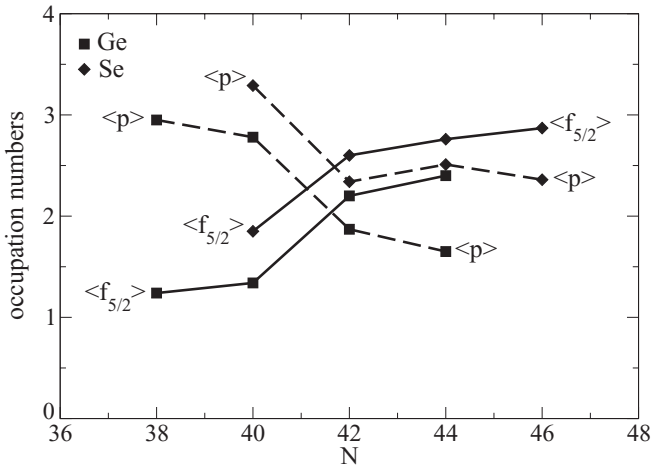

FIG. 12. Measured proton occupation numbers in the Ge and Se isotopes from Ref. [5]. Average global occupation numbers of the $2p_{3/2}$ and $2p_{1/2}$ orbitals (without distinction), $\langle p \rangle$, are connected with dashed lines and $\langle 1f_{5/2} \rangle$ with continuous lines.

rule out completely any possible prolate intrinsic shape. In addition, it is quite well and long established, mainly from the systematic study of Ge isotopes [6], that there is no experimental evidence of oblate intrinsic deformations beyond $N = 40$ just above $Z = 28$ (and no physical reason for their appearance). For that reason, it is quite clear that the structure transition from $N = 40$ to 42 can in no way be associated with the appearance of a rotational behavior connected with a permanently deformed intrinsic shape.

B. Possible microscopic origin of the collectivity development at $N = 42$ close to $Z = 28$

The first clue to the possible microscopic origin of the $N = 40$ to 42 transition can be sought in the impressive body of data from nucleon transfer experiments. Average proton occupations of the $1f_{5/2}$, $2p$, and $1g_{9/2}$ orbitals have been determined quite precisely in the Ge and Se chains [5,8,31] (see in particular Table 2 in Ref. [8] and Fig. 7 and Table 7 in Ref. [5]). Those numbers are represented in a graphical way in Fig. 12 for the sake of convenience. There is a clear change in the relative proton populations: from $N = 40$ to 42 approximately one proton is promoted on average from the $2p$ orbitals to $1f_{5/2}$. Though such precise data are not yet available for the Zn isotopic chain, one could imagine easily, due to the strong similitudes in the structure of the nuclei of the "S group," that the situation is likely to be the same also at $Z = 30$. We see no trivial explanation to this change of proton population: large-scale shell-model calculations show that proton $1f_{5/2}$ and $1p_{3/2}$ effective single-particle energies do cross, but at a higher number of neutrons (close to $N = 46$; see Fig. 1 in Ref. [40]). That would mean that some correlation effects are at play. For the sake of the present discussion, we just consider it as an empirical fact. Then the simplest explanation of the observed structure transition from $N = 40$ to 42 might originate from a Federman-Pittel-like phenomenon [41]. Since, as shown by all recent large-scale shell-model calculations, neutrons are already present in the $1g_{9/2}$ orbital before the $N = 40$ crossing, any increase of the population of an orbit with large orbital angular momentum, such as $1f_{5/2}$, would trigger the deformation driving proton-neutron interaction. $1g_{9/2}$ and $1f_{5/2}$ have equal radial number and $\Delta\ell = 1$. Furthermore, both have relatively large orbital angular momenta. Hence, following the ideas developed by Federman and Pittel, criteria for a strong proton-neutron interaction effect are indeed met. This should be enough to qualitatively explain the onset of collectivity (in the sense described above) from $N = 40$ to 42. In Ref. [3] the strong proton core polarization beyond $N = 40$ was already ascribed to the attractive $\pi 1f_{5/2}$-$\nu 1g_{9/2}$ monopole interaction.

In order to understand why the collectivity maximum at $N = 42$ reveals through γ-softness one should consider additional arguments. It is well known that the presence of orbitals, nearby the Fermi level, with high number of nodal planes parallel to the symmetry axis, $n_\perp$, broadens the potential curve in the γ coordinate. Here, $n_\perp = N - n_z$, where N and n_z are the principal quantum number and number of nodes along the symmetry axis in the $[Nn_z\Lambda]$ Nilsson labeling, respectively. In the beginning of a deformation region, all orbitals have low $n_\perp$ except those stemming from the lower shells, which, on the contrary have maximum $n_\perp$. In our specific case, this corresponds to the influence of the proton $7/2^-[303]$ orbital stemming from the underlying $1f_{7/2}$ spherical shell. In shell-model language, this simply means that the γ-softness observed here is a natural result of the influence of the breaking of the proton core.

Microscopic description of the ^{68}Ni region has recently reached a high degree of precision in the framework of the shell model. Impressive agreement between experimental and calculated magnetic moments of odd neutron-rich copper ground states has been achieved [40]. One of the major conclusions of Ref. [40] is that the only way to obtain such good agreement is by allowing proton core excitations (promotion of a proton from the $1f_{7/2}$ shell across the $Z = 28$ gap) in the calculations. An even larger valence space (pf-shell orbitals for protons and $f_{5/2}pg_{9/2}d_{5/2}$ orbitals for neutrons), allowing also neutron excitations across the $N = 50$ gap, has been used to account for the island of inversion phenomena in the neutron-rich Cr region [10]. A slightly revised version of the LNPS interaction of Ref. [10] was produced by Sieja and Nowacki [11] which allows improved agreement with the experimental $E(2^+)$, $B(E2)$ values, and $g(2^+)$ factors in the Zn isotopic chain [42]. A transition from $N = 40$ to $N = 42$ is also observed in the experimental g factors of the 2_1^+ states of Zn. The results of those calculations for the $B(E2)$ values are reported in Fig. 13. While the agreement is perfect up to $N = 40$ the theoretical curve is systematically shifted upward from $N = 42$ on. However, the maximum value, which should be, as deduced from the present experiment, at $N = 42$ is indeed reproduced. Interestingly enough, the modification of the LNPS interaction between Ref. [10] and Ref. [11] decreases the calculated $B(E2)$ value for the $N = 42$ isotone ^{70}Ni (degrading the agreement with experiment), while it is already too large for ^{72}Zn as only two protons are added. In Fig. 13, the results from calculations performed in the valence space restricted to $(1f_{5/2}2p_{3/2}1g_{9/2})$

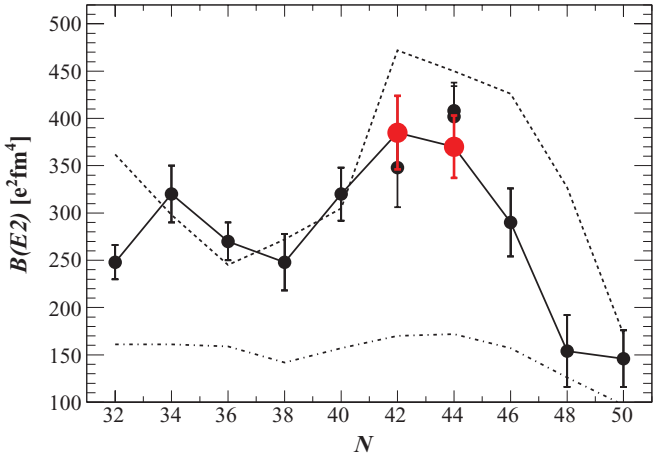

FIG. 13. (Color online) Experimental systematics of $B(E2)$ values for Zn isotopes compared to shell-model calculations using the LNPS interaction [11] (dotted line) and the JUN45 [9] (dash-dotted line) with standard effective charges ($e_p = 1.5e$ and $e_n = 0.5e$). New values available from the present work are represented in red. The solid line is to guide the eye.

using the JUN45 interaction [9] with standard effective charges ($e_p = 1.5e$ and $e_n = 0.5e$) are also reported for comparison. It is quite clear that the extension to the much larger valence space including also $\pi 1f_{7/2}$ and $\nu 2d_{5/2}$ represents a decisive improvement, being crucial for getting the necessary degrees of freedom and thus allowing the collectivity to develop at the correct magnitude. However, we hope that this discussion calls for a more careful balance of the collectivity which is brought in by the inclusion in the valence space of the like quadrupole partners $\nu g_{9/2}$-$\nu d_{5/2}$ with respect to the influence of the proton-neutron $\pi f_{5/2}$-$\nu g_{9/2}$ interaction and, to some extent, the influence of proton-core excitations.

V. SUMMARY

In summary, the lifetime measurement of the 2_1^+ states in ^{72,74}Zn has been performed at the LISE spectrometer at GANIL using the RDDS method. The lifetime values were determined to be 17.9(18) and 27.0(24) ps for ^{72}Zn and ^{74}Zn, respectively, which correspond to $B(E2; 2_1^+ \rightarrow 0^+) = 385(39)$ and 370(33) e^2 fm^4. The $B(E2)$ systematics obtained in the present work, when added to a careful inspection of other experimental quantities available for the neighboring nuclei, brings new support to the idea of a systematic maximum of collectivity at $N = 42$ for Zn, Ge, and Se nuclei. In addition, available signatures from the experimental spectra point toward a transition from a spherical oscillator at $N = 40$ to complete γ-softness at $N = 42$. From the whole body of data $Q(2_1^+)$ should be 0 for ^{72}Zn and close to it for ^{74}Zn, a value which is compatible with our data.

ACKNOWLEDGMENTS

We thank the GANIL staff for technical help and the EXOGAM Collaboration for providing the segmented-clover detectors. We also thank Dr. K. Sieja and Dr. F. Nowacki for providing us their recent calculations prior to their publication in Ref. [11]. This work was partially supported by the German BMBF (under Contract No. 06 DA 9040 I-1), the Polish Ministry of Science and Higher Education (Grants No. N N202 309135 and No. N N202 109936), and the Hungarian Scientific Research Fund (OTKA, Contract No. 100835).

[1] M. Bernas *et al.*, Phys. Lett. B **113**, 279 (1982).
[2] K. Langanke, J. Terasaki, F. Nowacki, D. J. Dean, and W. Nazarewicz, Phys. Rev. C **67**, 044314 (2003).
[3] O. Perru *et al.*, Phys. Rev. Lett. **96**, 232501 (2006).
[4] M. Vergnes *et al.*, Phys. Lett. B **72**, 447 (1978).
[5] G. Rotbard *et al.*, Nucl. Phys. A **401**, 41 (1983).
[6] R. Lecomte, M. Irshad, S. Landsberger, G. Kajrys, P. Paradis, and S. Monaro, Phys. Rev. C **22**, 2420 (1980); **22**, 1530 (1980).
[7] E. Nolte *et al.*, Z. Phys. **268**, 267 (1974).
[8] M. Vergnes, in *Proceedings of the Sixth European Physical Society Nuclear Divisional Conference on the Structure of Medium-Heavy Nuclei, Rhodes, Greece, 1979*, Institute of Physics Conference Series Vol. 49, edited by G. S. Anagnostatos, C. A. Kalfas, S. Kossionides, T. Paradellis, L. D. Skouras, and G. Vourvopoulos (Institute of Physics, Bristol, 1980), p. 25.
[9] M. Honma, T. Otsuka, T. Mizusaki, and M. Hjorth-Jensen, Phys. Rev. C **80**, 064323 (2009).
[10] S. M. Lenzi, F. Nowacki, A. Poves, and K. Sieja, Phys. Rev. C **82**, 054301 (2010).
[11] K. Sieja and F. Nowacki, arXiv:1201.0373v1.
[12] S. Leenhardt *et al.*, Eur. Phys. J. A **14**, 1 (2002).
[13] J. Van de Walle *et al.*, Phys. Rev. C **79**, 014309 (2009).
[14] A. Dewald *et al.*, Z. Phys. A **334**, 163 (1989).
[15] R. Anne *et al.*, Nucl. Instrum. Methods Phys. Res., Sect. A **257**, 215 (1987).
[16] Ch. Stodel *et al.*, in *Proceedings of the EXON* (World Scientific, Singapore, 2004), p. 180.
[17] S. Grévy and R. Hue, 24th World Conference of the International Nuclear Target Development Society - INTDS2008, Caen, France (2008).
[18] A. Dewald *et al.*, GSI Sci. Rep. 2005, 38 (2006).
[19] F. Azaiez and W. Korten, Nucl. Phys. News **7**, 21 (1997).
[20] G. de France and EXOGAM Collaboration, AIP Conf. Proc. **455**, 977 (1998).
[21] S. L. Shepherd *et al.*, Nucl. Instrum. Methods Phys. Res., Sect. A **434**, 373 (1999).
[22] O. H. Odland *et al.*, Nucl. Instrum. Methods Phys. Res., Sect. A **378**, 149 (1996).
[23] J. Allison *et al.*, IEEE Trans. Nucl. Sci. **53**, 270 (2006).
[24] S. Agostinelli *et al.*, Nucl. Instrum. Methods Phys. Res., Sect. A **506**, 250 (2003).
[25] J. H. Hamilton *et al.*, J. Phys. G: Nucl. Part. Phys. **10**, L87 (1984).
[26] T. Faul, Ph.D. thesis, University of Strasbourg, 2007.
[27] N. J. Stone, At. Data Nucl. Data Tables **90**, 75 (2005).
[28] K. Kumar, Phys. Rev. Lett. **28**, 249 (1972).

[29] R. Neuhausen *et al*., Nucl. Phys. A **263**, 249 (1976).
[30] N. V. Zamfir and R. F. Casten, Phys. Lett. B **260**, 265 (1991).
[31] M. Carchidi, H. T. Fortune, G. S. F. Stephans, and L. C. Bland, Phys. Rev. C **30**, 1293 (1984).
[32] H. T. Fortune and M. Carchidi, Phys. Rev. C **36**, 2584 (1987).
[33] B. Kotliński *et al*., Nucl. Phys. A **519**, 646 (1990).
[34] W.-T. Chou, D. S. Brenner, R. F. Casten, and R. L. Gill, Phys. Rev. C **47**, 157 (1993).
[35] Y. Toh *et al*., Eur. Phys. J. A **9**, 353 (2000).
[36] Y. Toh *et al*., J. Phys. G: Nucl. Part. Phys. **27**, 1475 (2001).
[37] M. Sugawara *et al*., Eur. Phys. J. A **16**, 409 (2003).
[38] J. Jabbour *et al*., Nucl. Phys. A **464**, 287 (1987).
[39] J. Reisberg *et al*., Nucl. Phys. A **280**, 13 (1977).
[40] K. Sieja and F. Nowacki, Phys. Rev. C **81**, 061303(R) (2010).
[41] P. Federman and S. Pittel, Phys. Lett. B **69**, 385 (1977); Phys. Rev. C **20**, 820 (1979).
[42] E. Fiori *et al*., Phys. Rev. C **85**, 034334 (2012).